Structure and Isomerization of an Intrastrand Cisplatin-Cross-Linked Octamer DNA Duplex by NMR Analysis†

Danzhou Yang,‡ Stella S. G. E. van Boom,§ Jan Reedijk,§ Jacques H. van Boom,§ and Andrew H.-J. Wang*,‡

Biophysics Division and Department of Cell & Structural Biology, University of Illinois at Urbana-Champaign, Urbana, Illinois 61801, and Leiden Institute of Chemistry, Gorlaeus Laboratory, Leiden University, 2300 RA Leiden, The Netherlands

Received April 10, 1995; Revised Manuscript Received July 13, 1995⊗

ABSTRACT: The anticancer platinum compound *cis*-$Pt(NH_3)_2Cl_2$ (cisplatin) forms covalent cross-linked adducts with DNA, with the intrastrand didentate adduct between two adjacent guanines being the major product. The platinum atom is coordinated at the N7 positions of adjacent guanines. The duplex consisting of d(CCTG*G*TCC) and its complement d(GGACCAGG), where G*G* stands for the cisplatin cross-linked lesion site, has been analyzed by 1D- and 2D-NMR spectroscopy and its structure solved by the NOE-restrained refinement procedure with the aim to understand the structural distortion associated with the lesion. The refined duplex is unwound (~−21°) and kinked (~58°) toward the major groove at the G*G* site, and the minor groove is significantly widened. The deoxyriboses of the G_4* and G_5* nucleotides are of the N-type (*C3′-endo*) and S-type (*C2′-endo*) conformations, respectively. The two guanine bases adopt the *R*-configuration (the α/β angles being 112°/290°, respectively), such that the G_5*H8 proton (upfield at 8.19 ppm) senses the ring current shielding effect of the G_4* base (G_4*H8 at 8.76 ppm). The G_4*•C_{13} base pair is perturbed significantly, consistent with the lack of detection of its imino proton. The *intra*strand Pt−G*pG* cross-link is metastable in the present DNA duplex. The molecule is slowly converted into a more stable *inter*strand didentate adduct (between G_4 and G_9) promoted by the presence of the nucleophilic chloride ion. The reason why the Pt−N7(3′-G*) bond can be ruptured and a new Pt−N7 bond formed may be due to the fact that the more flexible 5′-G*•C base pair at the didentate lesion site is able to absorb the strain better, but the more rigid 3′-G*•C base pair cannot and results in substitution. The biological implications of this structural isomerization are discussed.

The mode of action of the anticancer drug cisplatin (*cis*-diamminedichloroplatinum(II); also called *cis*-DDP; Figure 1) has been under intensive studies since its discovery 30 years ago (Rosenberg et al., 1965). This inorganic compound is remarkable. Despite its simple chemical structure, it is one of the most widely used anticancer drugs (Reedijk, 1992; Comess & Lippard, 1993). Its effectiveness against a number of cancers, particularly testicular cancer, is quite notable (Comess & Lippard, 1993).

The initial biologically-relevant events for the anticancer activity are associated with the formation of certain kinetically-stable platinum−DNA adducts. The kinetic process of this reaction has been probed (Bancroft et al., 1990). A major product (~70%) is the DNA lesion containing the (N7,N7)-didentate cisplatin cross-link between two intrastranded adjacent guanines. A lesser product is the intrastrand cross-link to the 5′-ApG sequence (15%). The remaining products consist of the intrastrand 1,3-cross-link to 5′-GXG sequences (Fichtinger-Schepman et al., 1985), the interstrand G to G cross-link at GpC sequence (Sip et al., 1992; Schwartz & Leng, 1994), as well as other minor adducts.

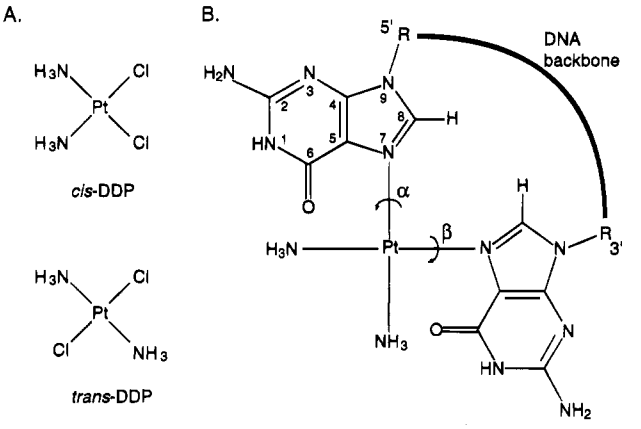

FIGURE 1: The chemical structures of (A) *cis*-diamminedichloroplatinium(II) (cisplatin; or *cis*-DDP) and *trans*-diamminedichloroplatinium(II) (*trans*-DDP) and (B) the intrastrand didentate cisplatin adduct with the GpG sequence.

The major intrastrand cross-links at the 5′-GpG and 5′-ApG sites have been suggested to be responsible for the biological activity of cisplatin. Such lesions have deleterious effects on replication and transcription (Corda et al., 1992) and cause mutations (Anderson, 1979; Bradley et al., 1993). Presumably, these biological effects are due to the structural distortion caused by the DNA lesions. However, it is

† This work was supported by NIH (GM-41612 and CA-52506) and American Cancer Society (DHP-114) grants to A.H.-J.W. and by the Netherlands Organization for Chemical Research (SON), with financial aid of the Netherlands Organization for the Advancement of Research (NWO), to J.R. and J.H.v.B. Additional support by the European Union (ERBCHRXCT920016) and by COST Action D1-92/002 (Biocoordination Chemistry) to J.R. and a NATO travel grant to J.R. and A.H.-J.W. are kindly acknowledged. The Varian VXR500 spectrometer at UIUC was supported by NIH Shared Instrumentation Grant 1S10RR06243.

* To whom correspondence should be addressed.
‡ University of Illinois at Urbana−Champaign.
§ Leiden University.

⊗ Abstract published in *Advance ACS Abstracts,* September 15, 1995.

0006-2960/95/0434-12912$09.00/0 © 1995 American Chemical Society

interesting to note that the other isomer of the platinum compound, *trans*-diamminedichloroplatinum(II) (*trans*-DDP), although capable of forming DNA adducts (Brabec et al., 1993), is not an effective anticancer drug. This difference in biological activities is clearly related to the different coordination geometry and has been the topic of intense research (Comess & Lippard, 1993). The cisplatin-induced DNA lesion is recognized by certain proteins whose binding to the lesion site may prevent the lesion from being repaired (Chao et al., 1991; Calsou et al., 1992; Chu, 1994). Such recognition is specific and it requires a "kinked" DNA conformation (Churchill & Travers, 1994). A number of those proteins have been identified and they contain the so-called "HMG box" domain (Pil & Lippard, 1992; Chow et al., 1995).

Elucidation of the structural distortion of the cisplatin−DNA adduct at the molecular level is an important step toward understanding the activity of cisplatin (Chu, 1994). NMR spectroscopy has become an increasingly useful means for structural studies. Earlier NMR work suggested that DNA duplex containing a single Pt−G*G*[1] lesion could be prepared and analyzed (den Hartog et al., 1985a,b). It was found that the base pair associated with the platinated 5′-G is destabilized. Later, a joint NMR and molecular mechanics study of a DNA duplex incorporating a Pt−G*G* lesion has generated several models in which the platinated DNA duplex was "kinked" with the helix axis bent ~60° toward the major groove at the Pt−G*G* site (Herman et al., 1990). This kink angle is larger than the estimated value of 35−40° derived from gel electrophoretic analysis of DNA duplexes with a varying number of bound cross-linked Pt atoms (Rice et al., 1988). The Pt-cross-linked DNA also has an unwinding angle of −13° as measured by the gel mobility of DNA (Bellon et al., 1991).

Attempts in getting the crystal structure of cisplatin−DNA adduct using oligonucleotides have had a limited success. The only crystal structures available thus far are those from the adducts between cisplatin and short ssDNA oligonucleotides, including d(pGpG) (Sherman et al., 1988; Coll et al., 1990) and d(CpGpG) (Admiraal et al., 1987). In the crystal structures cisplatin formed didentate adducts with the two adjacent Gs joined together in a "head-to-head" configuration, with the dihedral angles between the two Gs ranging from 75° to 82°. The deoxyribose at the 5′- and the 3′-dG nucleotides has the *C3′-endo* (N-type) and the *C2′-endo* (S-type) pucker, respectively.

In this paper, a detailed NMR structural analysis of the DNA duplex consisting of d(CCTG*G*TCC) and its complement d(GGACCAGG) is described. NOE-restrained refinements were carried out to arrive at a family of convergent models which afford a view of the structural distortion associated with the cisplatin lesion. In addition, the intrastrand Pt−GpG cross-link appears to be metastable in the present DNA duplex and may be converted into other adducts promoted by the nucleophilic chloride ion.

[1] Abbreviations: dsDNA, double-stranded DNA; ssDNA, single-stranded DNA; c^7G, 7-deazaguanine; G*G*, the cisplatin didentate intrastrand GpG cross-link; Intra-DX, cisplatin intrastrand didentate DNA adduct duplex; Inter-DX, cisplatin interstrand didentate DNA adduct duplex; NMR, nuclear magnetic resonance; 2D-NOESY, two-dimensional nuclear Overhauser effect spectroscopy; TOCSY, total correlated spectroscopy; rmsd, root-mean-squares deviation.

MATERIALS AND METHODS

Sample Preparation. Our target DNA molecule is a heteroduplex of the octamer sequence d($C_1C_2T_3G_4G_5T_6C_7C_8$) (denoted GG strand) and its complement d($G_9G_{10}A_{11}C_{12}C_{13}$-$A_{14}G_{15}G_{16}$) (denoted CC strand). The platinated DNA adduct of the GG strand was prepared by reacting in the dark a 0.05 mM GG strand solution in water with 1.2 equiv of cisplatin. The reaction was monitored by HPLC using a Mono-Q column run at pH 12. The GG strand appeared at a retention time of 12 min 43 s. After 10 h of reaction, the main product appeared at a retention time of 9 min 54 s. After a total of 4 days of incubation, the reaction was judged to be complete and stopped by ammonium hydrogen carbonate. The reaction mixture was loaded onto a Q-Sepharose Hiload™ 16/10 (Pharmacia) HPLC column for purification, and the desirable fractions were pooled, neutralized with acetic acid, and lyophilized. The purified Pt−DNA adduct was desalted using a Superdex-75 Hiload 16/120 (Pharmacia) gel filtration column. This gave the platinated DNA strand in 54.3% yield (14.07 mg) which is denoted G*G* strand. Two additional batches of the G*G* strand were similarly prepared.

The desired duplex has been prepared by titrating the CC strand into the solution of the G*G* strand. The precise ratio of the two strands was monitored using 1D-NMR spectra. As explained below, a total of five NMR samples were used for structural analysis. Sample 1 is the G*G* strand alone. Sample 2 has a 0.85:1 ratio of the CC strand to the G*G* strand. Sample 3 consists of an 1:1 ratio of the two strands, thus forming a clean duplex, designated as Intra-DX. Sample 4 and sample 5 are the products of sample 3 that have been left alone in the NMR tube for a few days and several weeks, respectively. These processes resulted in a mixture of the original Intra-DX and a new adduct (denoted Inter-DX) whose amounts increase with longer incubation time. Sample 5 is almost entirely Inter-DX. Separate Samples 2−5 were prepared both in D_2O and H_2O, respectively, for NMR analysis.

Electrospray mass spectrometry was performed using a FISONS/VG Quattro mass spectrometer at UIUC. One mg of desalted sample was dissolved in 1 milliliter of water and further diluted 4 times with water/2-propanol/0.4% NH_4-OH. Ten microliters of sample was injected via a Rheodyne 7125 valve into the flow system (50/50 acetonitrile/water) employing an ABI Model 140B pump at a flow rate of 10 μL/min. Data were acquired in the negative ion mode employing the VG MassLynx data system.

NMR Analysis. Typically, the NMR solution (5.65 mM duplex with 0.15 M NaCl and 0.05 M phosphate buffer at pH 7.0 in 0.55 mL of D_2O) of the platinated DNA oligomer was prepared using the established procedure (Robinson & Wang, 1992, 1993). NMR spectra were collected on a Varian VXR500 500 MHz spectrometer and processed with FELIX v1.1 (Hare Research, Woodinville, WA) on Silicon Graphics IRIS workstations. The temperature was controlled to be accurate within 0.01 °C. T_1 relaxation experiments were carried out with the standard 180°−τ−90° inversion−recovery sequence, and the average T_1 relaxation time is 2.2 s. The phase-sensitive NOESY spectra for nonexchangeable protons were recorded using the States/TPPI technique (States et al., 1982) for phase cycling. Homospoil pulses were used at the beginning of the recycling delay and at the

beginning of the mixing time. A total of 512 t_1 increments each with 2048 t_2 complex points were collected at a sweep width of 6000 Hz. Each FID was the average of 32 transients. The 2D NOESY data were collected at 2 °C with a mixing time of 110 ms and a total recycle delay of 4.9 s. The first FID was collected at a half-dwell delay to minimize the linear phase correction of the t_1 dimension. The preacquisition delay was empirically adjusted so that the linear phase correction for the t_2 dimension was minimized. The first point of each FID was multiplied by an empirical number to correct for the audio filter error; thus there was no need for the linear phase correction or base-line correction in either dimension. Apodization of the data in the t_1 and t_2 dimensions consisted of 8 Hz exponential multiplication with one half of a sine-squared function for the last one-fourth of the data to reduce truncation artifacts. In addition to 2D NOESY, standard TOCSY spectra were collected for the assignment of nonexchangeable protons.

2D-NOESY experiments for exchangeable protons were carried out for various samples in 90% H_2O/10 %D_2O using the 1−1 pulse sequence (Hore, 1983) as the read sequence (Sklenar et al., 1987a). The solvent signal is on-resonance. The offset was set to one-fourth of the sweep width (12 000 Hz) to get maximum excitation. Radiation damping effect was avoided using the method described by Sklenar et al. (1987b). Convolution of time-domain data was applied to improve solvent suppression (Marion et al., 1989). The resonances around 13 ppm were maximally excited. The mixing time was 150 ms and the recycle delay was 2.7 s for the 2D-NOESY spectra in 90% H_2O/10% D_2O, with the average of 16 transients. Chemical shifts were referenced to the HDO peak calibrated to a DSS standard at different temperatures.

Starting models of the platinated duplexes were built using QUANTA (version 4.0, MSI, Burlington, MA). The octamer duplex d(CCTG*G*TCC)·d(GGACCAGG) was constructed by extending the pG*pG* fragment which was obtained from the crystal structure of the cisplatin−pGpG adduct (Sherman et al., 1988). The model was energy-minimized using the steepest descent method in CHARMM (Brooks et al., 1983) with the atomic constraints (bond angle and bond length) of Pt atom and Pt-chelating nitrogens to fix the geometry of the Pt plane. The initial model was then introduced to X-PLOR (Brünger, 1992), and conjugate gradient minimization was performed. X-PLOR's all atom force field for DNA was used with explicit hydrogen bond potentials. The partial charges and the force constants of cisplatin and platinum-bound guanines were obtained from the molecular mechanics calculation by Herman et al. (1990) and from the X-PLOR package.

Integrals from the 2D NOE data set were extracted by evaluation with the observed crosspeak shapes of each spin in the f_1 and f_2 dimensions. These shapes were determined by spectral analysis with the program MYLOR (Robinson & Wang, 1992). Refinement of the starting model was carried out by the sequence of procedures comprising the SPEDREF package (Robinson & Wang, 1992). This includes a full-matrix relaxation calculation (Keeper & James, 1984) of the NOEs for the model with comparison of the experimental and simulated spectra to deconvolute overlapped areas of the spectra. Minimization of the residual errors within the program X-PLOR (Brünger, 1992) is then performed first by conjugate gradient minimization and then by simulated annealing (SA) with the NOE constraints. Forty cycles of SPEDREF refinement with conjugate gradient minimization followed by 10 cycles with SA were performed. The SA was run at 1000 K for 20 ps with weak NOE constraints in order to sample different conformations, then slowly cooled (10 K/100 fs) down to 0 K with strong NOE constraints. The isotropic correlation time (τ_c) for each refinement was empirically determined to be 15 ns. A family of converged models were obtained from the refinement with the R factor in the range of 15−16%.

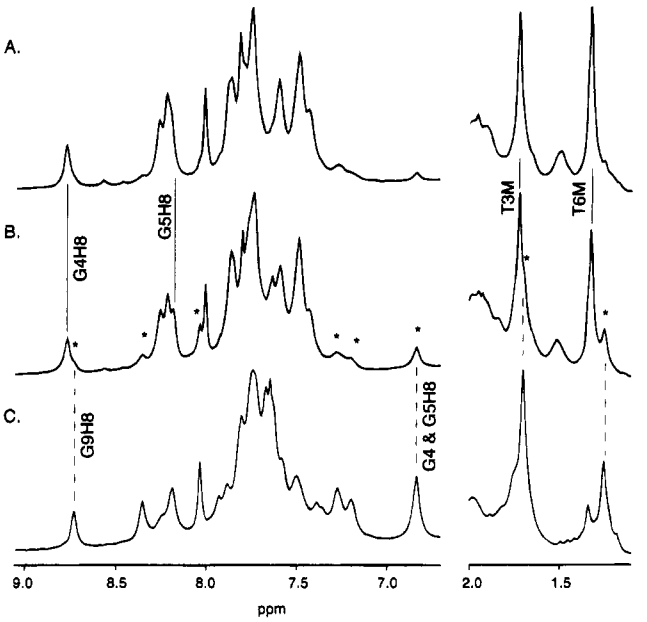

FIGURE 2: Titration of the CC strand to the G*G* strand as monitored by the methyl and aromatic regions of the 1D nonexchangeable proton NMR spectra recorded at 2 °C. (A) Sample 3: 1:1 ratio of CC strand to G*G* strand. (B) Sample 4: Solution of sample 3 after being stored in the NMR tube for several days. The new species is denoted with *. (C) Sample 5: Solution of sample 3 after being stored in the NMR tube for 2 months. The appearance and disappearance of several selected resonances from different molecular species are denoted by vertical lines.

RESULTS

Structural Analysis of the Cisplatin-Modified Duplex. The desired heteroduplex has been prepared by titrating the CC strand to the G*G* strand and monitoring the disappearance of the resonances (e.g., T methyl) derived from the G*G* strand. Figure 2 shows the methyl and aromatic regions of the 1D spectra at 2 °C. The average linewidth of the resonances is 20 Hz, which makes the quality of various COSY spectra inadequate for the measurement of the coupling constants.

2D-NOESY and TOCSY spectra in D_2O of sample 3 were used to assign the resonances of all nonexchangeable protons by standard DNA sequential assignment procedure (Figure 3). The connectivities of both strands are generally uninterrupted, with some variations in the intensity of the NOE crosspeaks from protons around the Pt−G_4*pG_5* lesion site. Figure S1 shows the complete 2D-NOESY spectra of Intra-DX. The chemical shifts of the assigned resonances are listed in Table 1. The 2D-TOCSY data (not shown) are consistent with the 2D-NOESY assignment. The chemical shifts of the G_4*H8 (8.76 ppm) and G_5*H8 (8.19 ppm) resonances are especially downfield, in comparison with

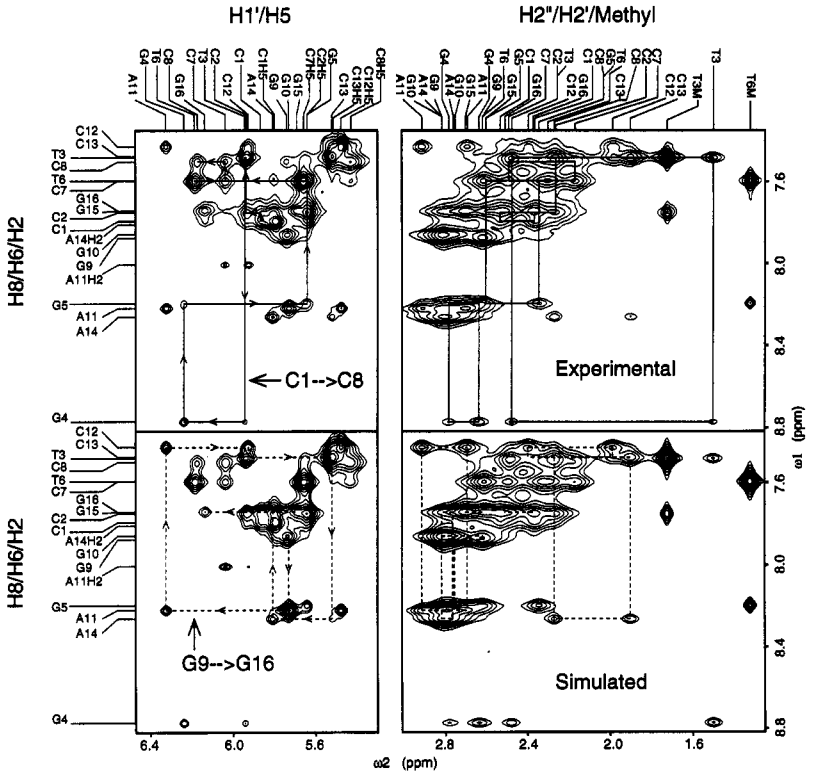

FIGURE 3: The expanded regions of the nonexchangeable proton 2D-NOESY spectra of Intra-DX (sample 3). (Left) Aromatic−H1′ region. (Right) Aromatic−H2′/H2″/methyl region. The simulated spectra based on the refined structure are shown in the bottom panels. The sequential assignment pathways of the two strands are shown separately with that from the C_1 to C_8 strand in solid lines (top panels) and that from the G_9 to G_{16} strand in dotted lines (bottom panels).

Table 1: ^{1}H Chemical Shifts of 5′-d(CCTG*G*TCC)•5′-d(GGACCAGG)[a]

	H6/H8	H5/H2/M	H1′	H2′/H2″	H3′	H4′	H5′/H5″	GH1/TH3	CH4/AH6
				Platinated Strand					
C1	7.79	5.79	5.87	2.37/2.53	4.64	4.11	3.79/3.79		7.91/6.92
C2	7.75	5.64	5.94	2.26/2.48	4.80	4.20	3.99/4.12		8.37/7.14
T3	7.48	1.73	5.94	1.50/2.48	4.82	4.12	4.20/4.20	14.41	
G4*	8.76		6.24	2.64/2.79	5.20	4.30	4.13/4.20		
G5*	8.19		5.64	2.35/2.61	4.64	4.26	4.16/4.11	13.24	
T6	7.59	1.33	6.18	2.31/2.62	4.91	4.30	4.15/4.11	14.05	
C7	7.59	5.66	6.04	2.17/2.49	4.85	4.16	4.20/4.25		8.58/7.14
C8	7.50	5.43	6.17	2.33/2.27	4.58	3.99	4.06/4.21		8.48/7.01
				Complementary Strand					
G9	7.87		5.74	2.62/2.82	4.86	4.26	3.69/3.73	13.00	
G10	7.85		5.73	2.76/2.82	5.06	4.42	4.12/4.22	12.92	
A11	8.21	8.00	6.32	2.70/2.92	5.05	4.48	4.13/4.31		8.10/6.17
C12	7.42	5.48	5.93	1.99/2.40	4.79	4.12	4.15/4.32		8.52/6.96
C13	7.47	5.52	5.52	1.90/2.27	4.80	4.06	3.99/4.20		8.13/6.93
A14	8.26	7.81	5.81	2.79/2.82	5.01	4.34	3.90/4.11		7.84/6.63
G15	7.74		5.69	2.61/2.71	5.00	4.41	4.12/4.16	12.93	
G16	7.73		6.14	2.52/2.37	4.67	4.26	4.13/4.13		

[a] G* is the platinated guanine residue. The stereospecific assignment has been made for H2′/H2″ protons, but not for H5′/H5″ protons.

other G resonances (7.70−7.78 ppm), indicating that both G_4* and G_5* bases are indeed platinated at their respective N7 positions. The intense G_4*H8−G_5*H8 crosspeak (Figure S2) further indicates that the two Gs are cross-linked by the cisplatin in a "head-to-head" configuration as that in the crystal structures (Sherman et al., 1988; Coll et al. 1990; Admiraal et al., 1987).

Interestingly, the crystal structures of the cisplatin−(pGpG) adduct revealed two classes of the "head-to-head" arrangement. They differ in the two torsional angles (α and β angles shown in Figure 1B) associated with the Pt−N7 bonds and are denoted as type R (right-handed) and type L (left-handed) configurations. The two G*H8 protons have distinct juxtapositions, which result in different chemical shifts for the 5′-G*H8 and 3′-G*H8 protons (Kozelka et al., 1992). In the R configuration the 5′-GH8 is more downfield than the 3′-GH8 proton, whereas the reverse is true for the L configuration. Figure S3 shows the two configurations (L in A and R in B) of the G*pG* site derived from the crystal structures (Sherman et al., 1988), with the complementary CpC sequence modeled in. Since G_4*H8 in the present molecule is more downfield, the cisplatin−G*pG* adduct should be in the R configuration.

A total of 1942 NOE crosspeak integrals were measured from the 2D-NOESY spectrum (Figure S1) by the procedure of MYLOR in the SPEDREF package (Robinson & Wang,

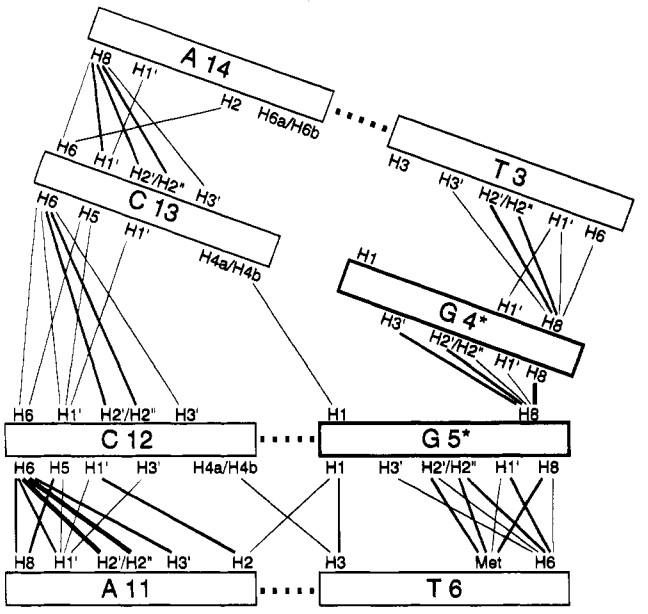

FIGURE 4: A schematic diagram showing important internucleotide NOE crosspeaks of Intra-DX whose intensities are represented by straight lines of varying thickness, denoting strong, medium, and weak NOE crosspeaks.

1992). Important internucleotide NOE crosspeak information is schematically summarized in Figure 4, which shows that a significant distortion exists at the Pt−G_4*pG_5* lesion site. The starting model prepared by the procedure described in Materials and Methods was subjected to a combined SPEDREF (Robinson & Wang, 1992) and NOE-constrained SA refinement (Brünger, 1992). Many cycles of refinement produced a family of converged models (all with an NMR *R* factor of ~15−16%). A view of one of the refined structures is shown in Figure 5. Other views are shown in Figure S4. The simulated NOESY spectra based on the refined model agree with the observed spectra (Figure S1). Some detailed comparisons between the calculated and the observed NOE crosspeaks are shown in Figure 3. To the best of our knowledge, this is the first detailed NOE-restrained refinement of an intrastrand cisplatin-cross-linked duplex. This is in contrast to earlier models which had been obtained through molecular mechanics modeling studies employing a limited number of NOE crosspeaks (Herman et al., 1990).

In the refined structure, the backbone conformation is significantly altered from B-DNA to accommodate the platination lesion. The compression in the major groove side makes the major groove deep and narrow, whereas a significant concomitant opening of the minor groove is noted (Figure S4). The strong intra-nucleotide G_4*H8−G_4*H3′ (peak B) and the modest G_5*H8−G_5*H3′ (peak C) crosspeaks (Figure S2) suggest that the deoxyriboses of the G_4* and G_5* nucleotides are of the N-type (*C3′-endo*) and S-type (*C2′-endo*) conformations. The complete torsion angles and the relevant conformational parameters of the refined duplex are listed in Tables S1 and S2, respectively. By inspecting the conformational parameters, our model seems to be similar to one of the models in the C_{0N} family proposed by modeling studies (Herman et al., 1990).

In the structure, the G_5*H8 proton remains underneath the imidazole ring of the G_4* base, therefore sensing the ring-current shielding effect of the G_4* base. As a result, the chemical shift of the G_5*H8 proton is more upfield (8.19 ppm) than that of G_4*H8 (8.76 ppm). Note that the C_{12}-pC_{13} step in the refined structure has a significantly smaller base pair opening (i.e., roll angle) than the starting models, which brings the C_{13} base closer to the G_5* base. This is corroborated by the unequivocal detection of the G_5*NH1−C_{13}NH4b crosspeak (peak R in Figure S5).

To address the question whether NMR NOE data are sufficient to arrive at convergent structures using different starting models, the following test was performed. Since the chemical shifts of G_4* and G_5* suggested that the configuration of the platinated G*pG* site is of the R type (Figure S3B), an alternative duplex model by starting with the L type Pt−G*pG* motif was built (Figure S3A) and refined. Refinement of the alternative model resulted in a refined structure (NMR *R* factor 16%) in which the Pt−G*pG* motif has reverted back to the R type configuration. The overall rmsd between the two refined structures (Figure S6) is 1.28 Å. Insofar as the NOE crosspeak intensities are concerned, the two structures may be considered converged. The refinement parameters of the two models are listed in Table S3.

Whether the G*G* and CC strands actually form a heteroduplex can be demonstrated directly by the presence of Watson−Crick base-paired imino protons. The exchangeable proton resonances were assigned by using the 2D-NOESY of the imino−imino region (Figure 6A) and the corresponding imino−amino and amino−aromatic regions (Figure S5) of the freshly-prepared sample 2. The G_4* imino proton is not observed, indicating that it is in rapid exchange

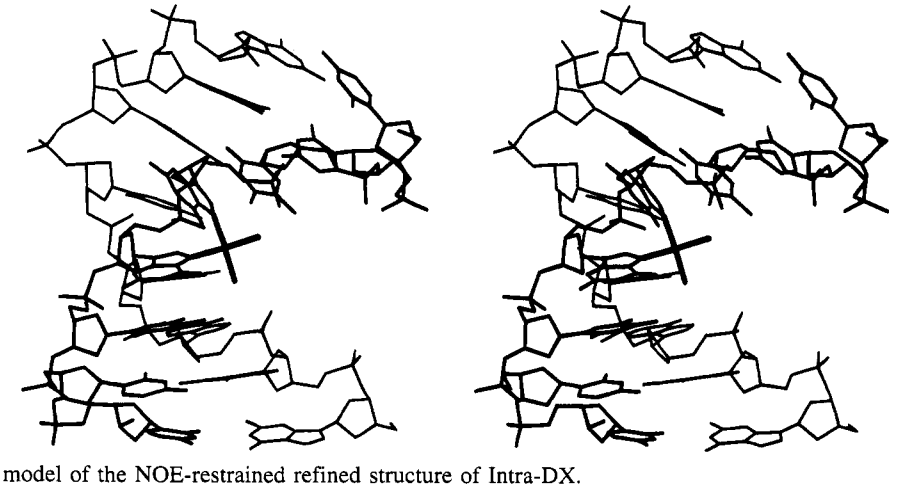

FIGURE 5: Molecular model of the NOE-restrained refined structure of Intra-DX.

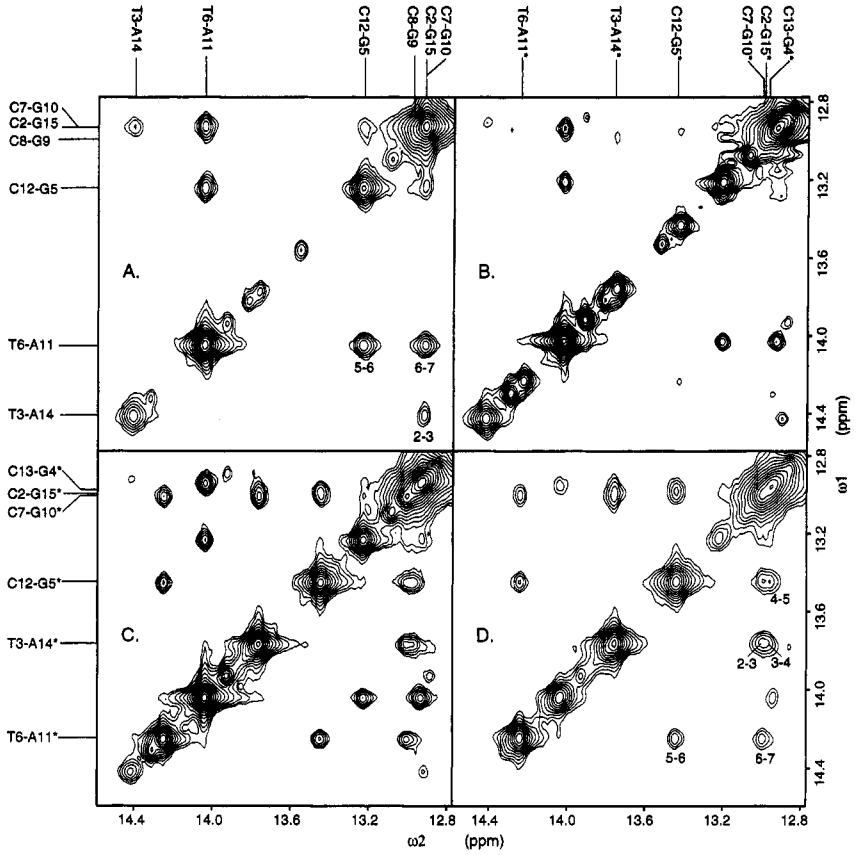

FIGURE 6: The exchangeable proton 2D-NOESY NMR spectra containing the imino-imino crosspeak region of different samples. (A) Freshly prepared sample 2. (B) Sample 3. Note that the G_4* and G_{16} imino protons are not visible. (C) Sample 4. (D) Sample 5. The numbers next to the crosspeaks identify the adjacent base pairs. The assignments for the imino protons of the two distinct samples (sample 2 for the Intra-DX and sample 5 (*) for Inter-DX) are labeled at the edges of the boxes.

with water protons. G_{16} imino proton of the terminal base pair is not observed either, likely due to fraying.

Isomerization between the Intra- and Interstrand Cisplatin−DNA Adducts. A curious phenomenon arose when the 2D-NOESY spectrum of sample 3 of Figure 2A was taken in H_2O, at 2 °C 1 day later. It revealed a major set and a minor set of imino/amino resonances (Figure 6B). After a few more days, the minor set of resonances (Inter-DX) became more prominent. The new T-methyl resonances, different from those of either the G*G* strand alone or the Intra-DX, emerge at 1.25 and 1.70 ppm (Figure 2B, sample 4). Similar changes occur elsewhere in the spectrum.

The observation of a significant second population of exchangeable NOE crosspeaks (Figure 6C, Sample 4), despite the fact that the nonexchangeable spectra showed only 25% contaminant (data not shown), is interesting. Figure 7 shows regions of the 1D spectra of the imino proton and the T-methyl resonances of an *aged* sample 4 on going from 5 to 40 °C. (This sample has been kept in the NMR tube for two more weeks than the sample 4 of Figure 2B.) Note that at 5 °C the methyl region has four (assigned) methyl peaks. Based on the peak areas, the ratio of Intra-DX to Inter-DX duplex is estimated about 60%:40%. Upon raising the temperature, the methyl resonances from Inter-DX (connected by solid lines) hardly moved, but those from Intra-DX (connected by dashed lines) moved significantly downfield toward the positions of ssDNA species. The imino resonances of Intra-DX completely vanished at ~15 °C, whereas those of Inter-DX persisted well beyond 30 °C, indicating that the latter is more stable. In addition, the Intra-DX is gradually turned into Inter-DX over time. By leaving the sample alone in the NMR tube for several weeks, Intra-DX is transformed entirely to Inter-DX (Figures 6D and 2C), as evident by the total disappearance of the characteristic methyl resonances of Intra-DX.

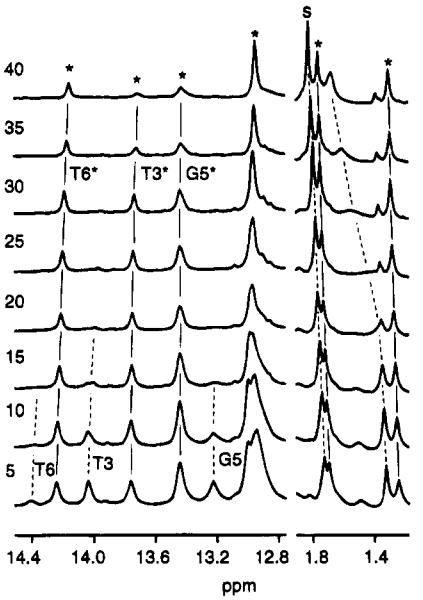

FIGURE 7: Temperature-dependent study of an aged sample 4 (see Figure 2B) monitored by the methyl (right) and imino (left) regions of the 1D exchangeable proton NMR spectra. The resonances from the interstrand didentate duplex are denoted by *, and they persist (even for the imino protons) at high temperature (40 °C).

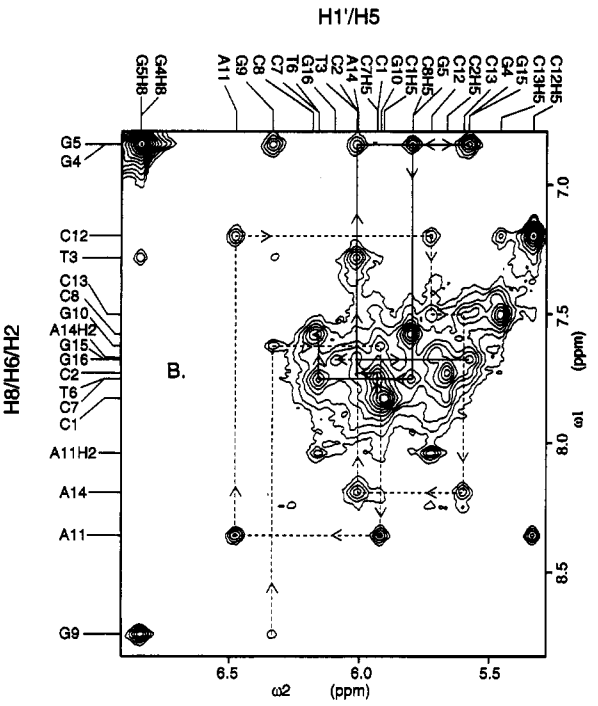

FIGURE 8: The expanded aromatic−H1′ region of the nonexchangeable proton 2D-NOESY spectrum of Inter-DX.

2D-NOESY and TOCSY spectra in D_2O at 2 °C for Inter-DX (sample 5) were used to assign all its resonances. It appeared to contain two products, with one product predominating (>90%) (Figure 2C). The identity of the new major product was determined to be that of an *inter*strand cisplatin-cross-linked octamer duplex (between G_4* and G_9*) as described below. Figure 8 shows the aromatic−H1′ region of 2D-NOESY at 2 °C, which contains important information of the structure. First, the G_9H8 is now the most downfield (8.73 ppm) resonance because the G_9* base is now platinated at N7. Both G_4H8 and G_5H8 resonances shifted to 6.83 ppm, substantially more upfield than that of the intrastrand chelated duplex, since the stacking of G_4* base over the G_5 base is affected by the highly distorted helical structure. Similar large upfield shifts are also observed for the G_4H2′/H2″ protons. Second, many resonances associated with the G_9 residue now have NOE crosspeaks to those from the T_3 and G_4 residues. For example, the G_9H8 to G_4H8 (but not to G_5H8) crosspeak is very intense, because the two bases are cross-linked. Third, clear base-to-base NOE crosspeaks in the $C_{12}pC_{13}$ step of the CC strand (i.e., C_{12}H6−C_{13}H5, C_{12}-H6−C_{13}H6 and C_{12}H5−C_{13}H6 crosspeaks), are readily detectable (not shown). It shows that the C_{12} is well stacked over C_{13}.

The unequivocal proof of its chemical structure came from the measured molecular mass of 5050 (calcd 5052) of sample 5 by electrospray mass spectrometry. Additional support comes from the HPLC profile of sample 5, which showed that the molecule now elutes at a slow retention time of 12 min and 50 s. (This retention time is similar to that from another interstrand cross-link between a DNA octamer CATGCATG with a bisplatinum (1,1/t,t) compound (Yang et al., 1995)).

The *inter*strand G_4* to G_9* cross-linked duplex (Inter-DX) is expected to be significantly more stable than Intra-DX. This is consistent with the imino proton spectra of various samples (Figures 6 and 7). Moreover, since the two duplexes are chemically different, there should be no NOE exchange crosspeak between the corresponding resonances. Again, our data support this. At present, the structural refinement of the interstrand didentate duplex is still in progress, and the results will be presented elsewhere.

DISCUSSION

Even though cisplatin has remarkable anticancer activities, it still has some shortcomings as all other anticancer drugs do. Among them, the side effect of toxicity and development of resistance by some cancer cells remain the major problems (Chu, 1994). Despite extensive efforts in the development of new Pt compounds which may avoid such problems, there is only one other compound, i.e., carboplatin, in clinical use (Knox et al., 1986; Blommaert et al., 1995). To help understand the mode of action of cisplatin, it is critical to know how cisplatin interacts with its major target of DNA. These include the sequence specificity, structural consequences of the formation of dsDNA−cisplatin adducts, the fate of the adducts, and binding of adducts with relevant proteins (Comess & Lippard, 1993).

The present studies here significantly augment earlier work by us and others and offer a new insight into the structure and stability of the cisplatin−DNA duplex adduct. The family of NOE-restrained refined structures of the cisplatin-modified duplex (one structure shown in Figure 5) showed that the helix is kinked (~58°) and unwound (~−21°), similar to earlier results of an exhaustive molecular mechanics computer modeling study (Herman et al., 1990). This kink angle value (~58°) is larger than that has been measured (~40°) by gel electrophoretic studies of the platinated DNA (Rice et al., 1988). To reconcile this discrepancy, the possible bendability associated with the Pt−N7 bonds may need to be considered (Guan et al., 1994). However, regardless what the kink angle is, the minor groove of the cisplatin-modified duplex has an enlarged groove width at the lesion site (Figure S4). It is reasonable to believe that such structural features shown in Figure 5 are the recognition motifs for proteins (e.g., HMG box domain) that bind cisplatin-lesioned DNA.

In the past, the stability of the cisplatin−G*pG* adduct has not been systematically studied. Although it is well-known that the Pt−N7 bonds can be reverted by stronger nucleophilic ligands such as CN^- ion (Decoville et al., 1993), it is not entirely clear how inert those bonds are, nor the relative stability of the two Pt−N7 bonds. Some recent studies showed that under certain circumstances the monofunctional Pt−N7(G*) bond can be exchanged with other Pt−N bonds where the nitrogen is from certain pyrimidine or pyridine moieties (Payet et al., 1993). Here, we show that the intrastrand cisplatin-cross-linked octamer duplex is metastable. The process with which the Pt−N7(3′-G*) bond can be ruptured and a new Pt−N7 bond formed is presumably mediated by the chloride ion, since the process did not occur in the absence of Cl^- (not shown). Mechanistically, the Cl^- ion may attack the platinum atom (from an axial position on the square coordination plane) as the first step. However, understanding the detailed mechanism requires further study.

The new finding on the instability of Intra-DX may have many biological ramifications. For example, can the same reaction be carried out *in vivo* by other nucleophilic

biological ligands (e.g., thiol or amine group from proteins)? If the Pt−N7 bond can be broken at one place and re-formed at another place, is it possible that the platinum atom may "migrate" on a DNA duplex? This may be tested.

Why is the Pt−N7(3′-G*) bond less stable than the Pt−N7(5′-G*) bond? This may be related to the relative flexibility of the two platinated G nucleotides. The imino proton 2D-NOESY of Intra-DX indicated that the G_4*•C_{13} base pair is less ordered (i.e., more flexible) since its imino proton could not be detected (Figure 6). In contrast, the imino proton of the G_5*•C_{12} base pair (at 13.24 ppm) is readily observed, implying a more rigid structure. In fact, the 2D-NOESY data suggest that the duplex toward the 3′-end (including the G_5*•C_{12}, T_6•A_{11}, C_7•G_{10}, and C_8•G_9 base pairs) is more ordered than the 5′-end. It is possible that the more flexible 5′-G*•C base pair at the lesion site is able to dissipate better the strain caused by the Pt lesions, but the more rigid 3′-G*•C base pair cannot. This hypothesis may be tested with molecular mechanics calculation/molecular dynamics simulation.

The lability of the Pt−N7(3′-G*) bond in Intra-DX offers some clues on the sequence preference for the cisplatin attack on DNA. The principal targets for cisplatin and carboplatin are the GpG site and, to a lesser extent, the ApG site, but not the GpA site (Fichtinger-Schepman et al., 1985; Inagaki et al., 1988; Blommaert et al., 1995). From only the structural point of view, it is difficult to understand what is the difference between ApG and GpA sites. Some have suggested that the NH_3 ligand forms a hydrogen bond to the O6 atom of the 3′-G, which may stabilize the structure. However, the refined structures do not show such hydrogen bonds. An alternative explanation may be the following. If the Pt−N7(3′-G*) bond in the GpG or ApG sites would be labile, the corresponding Pt−N7(3′-A*) bond in a GpA site would be even more labile since the N7 of A is less nucleophilic than that of G. Therefore, the transient formation of a didentate cisplatin adduct at the 5′-GpA site is likely to have its Pt−N7(3′-A*) bond ruptured easily and might be transformed into other more stable adducts, including the interstrand didentate adducts.

In sample 5 the major species is that of the G_4 (of the GG strand) and the G_9 (of the CC strand) interstrand cross-link. Why G_9? The distances between the Pt atom and the G_{10}-N7 and G_9N7 atoms in Intra-DX (Figure 5) are 9.02 and 12.64 Å, respectively. It is possible that since G_9 is a terminal nucleotide (therefore having a greater flexibility), it is able to swing around and attack the Pt atom using its N7 site more easily. The minor species in sample 5 may be the G_4-to-G_{10} interstrand adduct; this product is also very stable (data not shown). It should be noted that the other two Gs (G_{15} and G_{16}) in the CC strand are in an unfavorable position to react with the Pt atom.

The ability of cisplatin to form interstrand didentate adducts has attracted recent attention (Sip et al., 1992). Lemaire et al. (1991) have shown that the preferred binding site for the interstrand cross-link is at a GpC step. Recently, it has been shown that in the sequence of CGCGGG cisplatin forms an unexpected interstrand adduct, rather than the expected intrastrand adduct at a GG site (Zou et al., 1994). Whether our data on the lability of the intrastrand GG adduct here bear direct relevance to such observations remains to be determined.

A number of other issues remain to be resolved. It will be important to know whether the stability of the cisplatin−GpG adduct is dependent on the sequence contexts. In the present octamer sequence, the cisplatin−G*pG* adduct is sandwiched between two A•T base pairs. Intuitively, one assumes that the cisplatin−G*pG* lesion here is under less strain than if it is sandwiched between two stronger G•C base pairs. Therefore, the G*G* site in the C(G*G*)C sequence may be less stable than that in the T(G*G*)T sequence. In other words, the Pt−N7(3′-G*) bond in the former sequence may be more prone to be ruptured. The cisplatin−GpG adduct is known to induce mutation, mostly transversion (Bradley et al., 1993). This may be related to the instability of the base pairs associated with the two guanines. It would be of interest to investigate the stability of duplexes with different bases (e.g., A instead of C) opposite the guanines.

It is clear that a cisplatin didentate lesion introduces significant instability to the DNA duplex. There are a number of ways that DNA can change conformation to attain more stability. For example, if the Pt−G*pG* site is embedded in an inverted repeat sequence, the DNA may adopt a hairpin structure, as has recently been shown for the palindromic sequence (ATGG*G*TACCCAT) (Yohannes et al., 1993; Iwamoto et al., 1994). In the latter structure, the platinated G_4*pG_5* site is incorporated into the loop, with the 3′-side G_5* adopting the *syn* conformation. Similarly, we have noted that in the cisplatin-cross-linked adduct of d([c^7A]CC[c^7G][c^7G]CCG*G*T) the G_9* is also in the *syn* conformation (unpublished data). The Pt−N7 bond of the Pt−G*G* adduct in this molecule appears to be more stable, since treatment of this decamer DNA with Cl^- ion did not damage any of the Pt−N7 bonds (unpublished data). This may be related to the fact that the CG*G*T segment at the 3′-end appears to have mostly ssDNA characteristics on the basis of our NMR analysis. Therefore, it is concluded that the cisplatin−GG adduct may only become unstable when it is in a duplex environment.

ACKNOWLEDGMENT

We thank Mr. H. van den Elst for his technical assistance and Johnson & Matthey (Reading, U.K.) for their generous loan of K_2PtCl_4. The Leiden part of the work has been performed under the auspices of the joint BIOMAC Research Graduate School of Leiden University and Delft University of Technology.

SUPPORTING INFORMATION AVAILABLE

Three tables listing the torsion angles, conformational parameters of the refined structure, and refinement parameters, plus six figures showing the complete experimental and calculated 2D-NOESY spectra, expanded regions of the 2D-NOESY spectra in D_2O and H_2O of the G*G*•CC intrastrand duplex, various conformations of the Pt−G*pG* site, and comparisons of the structures from two starting models (12 pages). Ordering information is given on any current masthead page.

REFERENCES

Admiraal, G., Van der Veer, J. L., de Graaff, R. A. G., den Hartog, J. H. J., & Reedijk, J. (1987) *J. Am. Chem. Soc. 109*, 592−594.

Anderson, K. S. (1979) *Mutat. Res. 67*, 209−214.

Bancroft, D. P., Lepre, C. A., & Lippard, S. J. (1990) *J. Am. Chem. Soc. 112*, 6860−6871.
Bellon, S. E., Coleman, J. H., & Lippard, S. J. (1991) *Biochemistry 30*, 8026−8035.
Blommaert, F. A., van Dijk-Knijnenburg, H. C. M., Dijt, F. J., den Engelse, L., Baan, R. A., Berends, F., & Fichtinger-Schepman, A. M. J. (1995) *Biochemistry 34*, 8474−8480.
Brabec, V., Sip, M., & Leng, M. (1993) *Biochemistry 32*, 11676−11681.
Bradley, L. J. N., Yarema, K. J., Lippard, S. J., & Essigmann, J. M. (1993) *Biochemistry 32*, 982−988.
Brooks, B. R., Bruccoleri, R. E., Olafson, B. D., States, D. J., Swaminathan, S., & Karplus, M. J. (1983) *Comput. Chem. 4*, 187−217.
Brünger, A. T. (1992) *X-PLOR*, version 3.1, Yale University, New Haven, CT.
Calsou, P., Frit, P., & Salles, B. (1992) *Nucleic Acids Res. 20*, 6363−6368.
Chao, C. C.-K., Huang, S.-L., Lee, L.-Y., & Lin-Chao, S. (1991) *Biochem. J. 277*, 875−878.
Chow, C. S., Barnes, C. M., & Lippard, S. J. (1995) *Biochemistry 34*, 2956−2964.
Chu, G. (1994) *J. Biol. Chem. 269*, 787−790.
Churchill, M. E. A., & Travers, A. A. (1994) *Trends Biochem. Sci. 19*, 185−187.
Coll, M., Sherman, S. E., Gibson, D., Lippard, S. J., & Wang, A. H.-J. (1990) *J. Biomol. Struct. Dyn. 8*, 315−330.
Comess, K. M., & Lippard, S. J. (1993) in *Molecular Aspects of Anticancer Drug-DNA Interactions* (Neidle., S., & Waring, M., Eds.) pp 134−168, Macmillan Press, London.
Corda, Y., Anin M.-F., Leng, M., & Job, D. (1992) *Biochemistry 31*, 1904−1908.
Decoville, M., Schwartz, A., Locker, D., & Leng, M. (1993) *FEBS Lett. 323*, 55−58.
den Hartog, J. H. J., Altona, C., van der Marel, G. A., & Reedijk, J. (1985a) *Eur. J. Biochem. 147*, 371−379.
den Hartog, J. H. J., Altona, C., van Boom, J. H., van der Marel, G. A., Haasnoot, C. A. G., & Reedijk, J. (1985b) *J. Biomol. Struct. Dyn. 2*, 1137−1155.
Fichtinger-Schepman, A. M. J., van der Veer, J. L., den Hartog, J. H. J., Lohman, P. H. M., & Reedijk, J. (1985) *Biochemistry 24*, 707−713.
Guan, Y., Gao, Y.-G., Liaw, Y.-C., Robinson, H., & Wang, A. H.-J. (1993) *J. Biomol. Struct. Dyn. 11*, 253−276.
Herman, F., Kozelka, J., Stoven,V., Guittet, E., Girault, J.-P., Huynh-Dinh, T., Igolen, J., Lallemand, J.-Y., & Chottard, J.-C. (1990) *Eur. J. Biochem. 194*, 119−133.
Hore, P. J. (1983) *J. Magn. Reson. 54*, 539−542.
Inagaki, K., Tomita, A., & Kidani, Y. (1988) *Bull. Chem. Soc. Jpn. 61*, 2825−2831.
Iwamoto, M., Mukunda, S. J., & Marzilli, L. G. (1994) *J. Am. Chem. Soc. 116*, 6238−6244.
Keeper, J. W., & James, T. L. (1984) *J. Magn. Reson. 57*, 404−426.
Knox, R., Friedlos, F., Lydall, D., & Roberts, J. (1986) *Cancer Res. 46*, 1972−1979.
Kozelka, J., Fouchet, M.-H., & Chottard, J.-C. (1992) *Eur. J. Biochem. 205*, 895−906.
Lemaire, M. A., Schwartz, A., Rahmouni, A. R., & Leng, M. (1991) *Proc. Natl. Acad. Sci. U.S.A. 88*, 1982−1985.
Marion, D., Ikura, M., & Bax, A. (1989) *J. Magn. Reson. 84*, 425−430.
Payet, D., Gaucheron, F., & Leng, M. (1993) *Nucleic Acids Res. 21*, 5846−5851.
Pil, P. M., & Lippard, S. J. (1992) *Science 256*, 234−237.
Reedijk, J. (1992) *Inorg. Chim. Acta 198−200*, 873−881.
Rice, J. A., Crothers, D. M., Pinto, A. L., & Lippard, S. J. (1988) *Proc. Natl. Acad. Sci. U.S.A. 85*, 4158−4161.
Robinson, H., & Wang, A. H.-J. (1992) *Biochemistry 31*, 3524−3533.
Robinson, H., & Wang, A. H.-J. (1993) *Proc. Natl. Acad. Sci. U.S.A. 90*, 5224−5228.
Rosenberg, B., Van Camp, L., & Kirgan, T. (1965) *Nature 205*, 698.
Schwartz, A., & Leng, M. (1994) *J. Mol. Biol. 236*, 969−974.
Sherman, S. E., Gibson, D., Wang, A. H.-J., & Lippard, S. J. (1988) *J. Am. Chem. Soc. 110*, 7368−7381.
Sip, M., Schwartz, A., Vovelle, F., Ptak, M., & Leng, M. (1992) *Biochemistry 31*, 2508−2513.
Sklenar, V., Brooks, B. R., Zon, G., & Bax, A. (1987a) *FEBS Lett. 216*, 249−252.
Sklenar, V., Tschudin, R., & Bax, A. (1987b) *J. Magn. Reson. 75*, 352−357.
States, D. J., Haberkorn, R. A., & Ruben, D. J. (1982) *J. Magn. Reson. 48*, 286−292.
Yang, D.,van Boom, S. S. G. E., Reedijk, J., van Boom, J. H., Farrell, N., & Wang A. H.-J. (1995) *Nat. Struct. Biol. 2*, 577−586.
Yohannes, P. G., Zon, G., Doetsch, P. W., & Marzilli, L. G. (1993) *J. Am. Chem. Soc. 115*, 5105−5110.
Zou, Y., van Houten, B., & Farrell, N. (1994) *Biochemistry 33*, 5404−5410.

BI950807H